Journal of Particle Science and Technology 10 (2) (2024) 87-96

Iranian Research Organization for Science and Technology (IROST)

Journal of PARTICLE Science & Technology

JPSIT
https://jpst.irost.ir

Online ISSN: 2423-4079
Print ISSN: 2423-4087

Ultrasonic assisted cold compaction of CP titanium and Ti-6Al-4V alloy

Vahid Fartashvand[✉,1], **Rezvan Abedini**[2], **Raheleh Khanmohammadi**[3], **Amir Abdullah**[3], **Nader Parvin**[4]

[1] *Department of Industrial Design, Faculty of Art, Alzahra University, Tehran, Iran*
[2] *Department of Mechanical Engineering, University of Science and Technology, Tehran, Iran*
[3] *Department of Mechanical Engineering, Amirkabir University of Technology, Tehran, Iran*
[4] *Materials and Metallurgical Engineering Department, Amirkabir University of Technology, Tehran, Iran*

HIGHLIGHTS

- The multi-particle finite element method (MPFEM) was used to simulate ultrasonic-assisted cold compaction of CP-Ti and Ti-6Al-4V.
- Acoustic softening was studied for each material.
- Friction reduction due to ultrasonic vibration was investigated.
- Reduction of compaction pressure was recorded while applying ultrasonic vibration.
- Higher particle rearrangement and plastic deformation were found due to

GRAPHICAL ABSTRACT

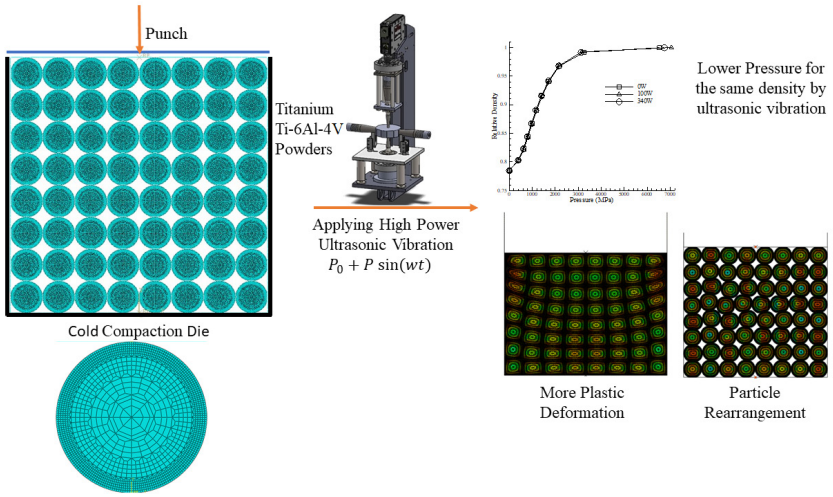

ARTICLE INFO

Article type:
Research article

Article history:
Received 8 September 2024
Received in revised form 10 November 2024
Accepted 18 November 2024

Keywords:
Multi-particle finite element
Cold consolidation
High power ultrasonic vibration
Acoustic softening

DOI: 10.22104/jpst.2024.7089.1262

ABSTRACT

Superimposed ultrasonic vibration during compaction of commercially pure (CP) titanium and Ti-6Al-4V alloy improves the relative density and quality of the compact. The underlying mechanisms of this process are not well understood. In this study, the influence of ultrasonic vibrations on the densification behavior of square packing of Ti-6Al-4V and CP-Ti powders during cold compaction was investigated using the Multi-Particle Finite Element Method (MPFEM). Acoustic softening and friction reduction were introduced in this model. The density-pressure curves show that ultrasonic vibration improves the densification of these powders, owing to the acoustic softening that leads to a decline in the required pressure. It has been found that the ultrasonic effect on reducing the compaction pressure and stress in the case of pure titanium is greater than that of titanium alloy. In addition, an increase in the intensity and amplitude of ultrasonic vibration reduces stress. The rotation and rearrangement of the particles caused by the reduction of friction lead to an enhancement in the compression capability.

✉ *Corresponding author: E-mail address:* v.fartashvand@alzahra.ac.ir ; *Tel:* +9821-88035801

1. Introduction

Titanium and its alloys have advantageous properties such as high specific strength, high corrosion resistance, and biocompatibility. Therefore, they are widely used in the chemical, medical, aero, and jewelry industries [1,2]. Due to the high cost of these materials, powder metallurgy (PM) is a near-net-shape manufacturing technology that has been widely used to fabricate components [3,4]. In addition, easy operation and a high production rate are other advantages of PM technology. Press and sintering is the most straightforward technology among powder metallurgy techniques [5]. In this operation, the powder is pressed into a desirable shape, and then the compacted part is sintered. Inter-particle friction and die wall friction decrease the effective pressure along with the component thickness, and this pressure gradient induces inhomogeneous density distribution in compacted bodies.

Shape distortion after sintering is the main result of this density variation. To overcome this problem, ultrasonic vibration has been successfully superimposed on the compaction of titanium powders [6-8]. Ultrasonic vibration causes the reduction of friction force at contacting surfaces [9] and diminishes the pressure gradient along the compacted part. In addition, the reduction of flow stress during superimposing ultrasonic vibration (called acoustic softening) decreases forming forces [10]. As another benefit, heat generation at the contacting surface due to absorption of ultrasonic vibration increases the compressibility of powders [11-13]. These advantages incentive using ultrasonic vibration during powder consolidation of low compressibility powders. Therefore, any improvement in the compaction processes of powders leads to high-quality compacted parts and thus increases the mechanical properties of the final piece.

Densification of the powder mass depends on various parameters such as the elastic-plastic properties of particles, the size and morphology of particles, the particle configuration, the inter-particle friction, the friction between the particles and the die walls, and loading. The role of each parameter on the powder densification behavior is not easily obtainable in experimental tests due to their interaction. Also, compaction pressure, lubricant, sintering temperature, and sintering time [14,15] are the main parameters of the powder compaction process. The relative density of the titanium green compact is directly proportional to the compaction pressure. These frictional effects can be reduced by the use of suitable lubricant [16]. Sintering is one of the most critical steps of powder metallurgy. The time and temperature of the sintering, the sintering atmosphere, and the heating rate could influence the compacted part's mechanical properties.

Numerical modeling, which has the ability to modify a parameter according to the intended behavior, is valuable for understanding densification mechanisms. Two basic procedures have been used for the numerical modeling of the powder compaction process, namely the discrete element method (DEM) and the finite element method (FEM). In DEM, each particle is modeled, and Newton's laws calculate the adjacent particle's interaction. Contact and separation between the particles are detected by progressing the compaction process. In FEM, the porous constitute equation of material is considered, but the rotational spin and particle rearrangement are ignored [17]. In recent years, the multi-particle finite element method (MPFEM) has been proposed and used to simulate powder compaction. The advantage of MPFEM lies in that it combines the features of traditional FEM and DEM and can successfully simulate the compaction densification of powders with large deformation from a particulate scale [18,19]. The MPFEM method is modeled as deformable continuum material, and their interactions are considered. The interaction between the neighboring particles is calculated based on DEM, and their deformation is calculated with FEM.

Many research studies have been conducted on powder compaction using an MPFEM. Procopio *et al.* applied the MPFEM approach to investigate the multi-axial condensation of granular mass from weak to high relative densities in 2D [17]. Their work demonstrates that the MPFEM model is beneficial in explaining inter-particle behavior and its impact on the microscopic and macroscopic response in different strain histories. Kim *et al.* used the MPFEM method to observe the deformation behavior of aluminum particles and estimate the relative density for different punch speeds and particle diameters [20]. Huang *et al.* used MPFEM to numerically study the 2D compaction of binary Al/SiC composite powders [18]. They constructed different initial packing structures with various Al/SiC particle size ratios and compositions and imported them into a FEM model for compaction. Their results show that initial powder packing configurations determine the densification process and the properties of the compacts. Mei *et al.* simulated the densification of Al and NaCl powders by CZM-based MPFEM [21]. They simulated the fracture of particles using this method. Han *et al.* simulated 2D compaction of Fe-Al composite powders by MPFEM at different size ratios [22]. Korim and Hu studied spongy copper powder densification and compaction mechanisms using a multi-particle finite element method [19]. Zhou *et al.* used MPFEM to determine green density and impact energy relation in Ti-6Al-4V powders [23]. Ji *et al.* simulated the hot-pressing densification of (SiCp)/6061Al composite powders [24]. In this study, the influence of ultrasonic vibration on the compaction of Ti-6Al-4V and CP-Ti was investigated by computer simulation.

This study is a part of our investigation on ultrasonic-assisted powder cold/hot compaction. Until now, no study on the MPFEM of ultrasonic-assisted compaction has been published. Therefore, this study focuses on mono-size circular particles to investigate the influence of ultrasonic vibration (acoustic softening and friction reduction) on compaction efficiency. A better understating of ultrasonic-assisted cold compaction will improve green part quality and, therefore, increase final product quality.

2. Simulation Procedure and Condition

This simulation analyzed the densification behavior of particles under uniaxial pressing without ultrasonic vibration and with superimposed ultrasonic vibration using MPFEM. The simulation was conducted using finite element software ABAQUS/Explicit. An explicit integration scheme was used because it is appropriate for contact problems and a high degree of freedom systems. Also, the system is modeled as a two-dimensional plane strain. Selecting the desirable mesh (size and type) is an essential step in finite element numerical modeling. Different mesh types and sizes were used (as shown in Fig. 1). In a mesh sensitivity study, a deformable particle is modeled between upper and lower punches to decrease simulation cost. Then, by applying compression force at the rigid upper punch, the force-displacement curve (Fig. 2) and Von Mises effective stress (Fig. 3) were extracted. A transient mesh (as shown in Figure 1-H) was chosen based on simulation cost and accuracy.

In the next step, the simulation's accuracy was investigated using Wu *et al.* experimental work [14]. Xin *et al.* results have been used to verify the simulation shown in Fig. 4 [28]. As shown from these curves, there is a good agreement between simulation and experimental data. So, the modeling procedure was shown to have significant accuracy in simulating a collection of particles. Since a large mesh size causes fluctuation in this curve, a smooth curve indicates a suitable mesh size.

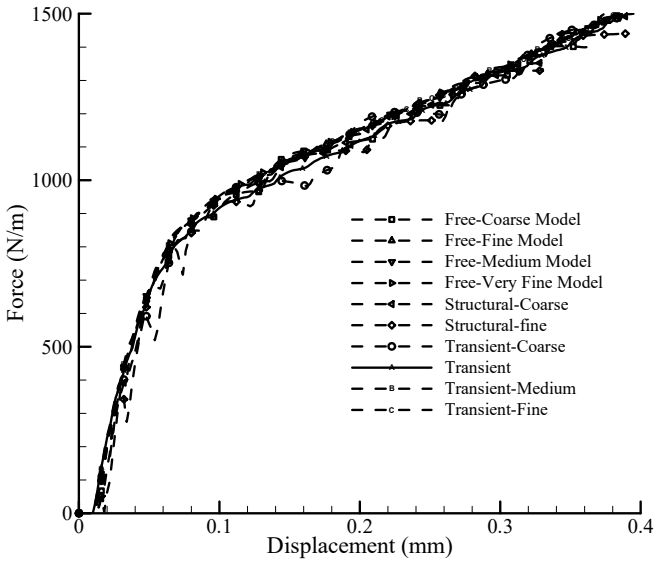

Fig. 2. The effect of mesh size and type on force-displacement curves of the upper punch.

Finite-discrete element modeling has many computations due to the existence of many distinct particles with different geometry and nonlinear behavior, namely elastic-plastic deformation and the presence of many contact surfaces. In this study, a cylindrical die with 12 mm diameter and 12 mm height was modeled. The number of particles that can be modeled is determined by CPU and RAM restrictions and the number of particle-particle contact pairs. Therefore, 64 circular particles with a diameter of 1.5 mm were considered

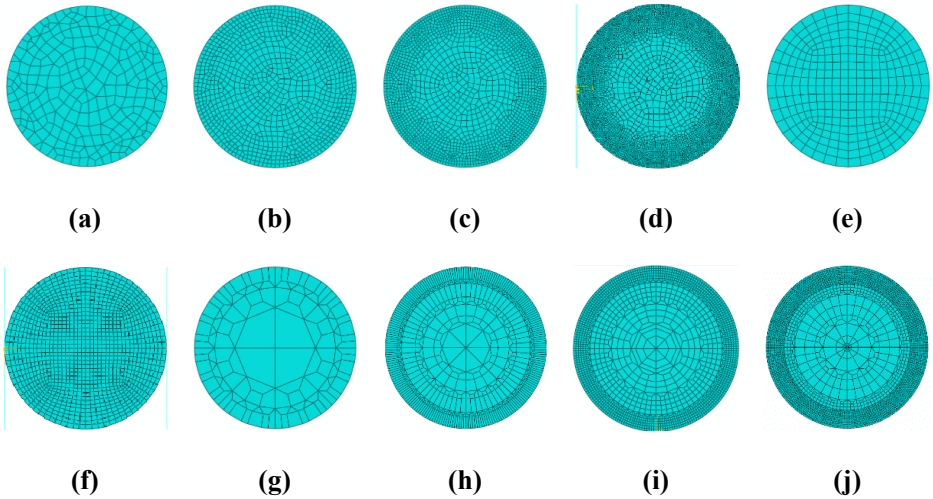

Fig. 1. Mesh sensitivity analysis: (a) Coarse free mesh, (b) Medium free mesh [25], (c) Fine free mesh, (d) Very fine free mesh, (e) Coarse structural mesh [26], (f) Fine structural mesh, (g) Coarse transient mesh [9], (h) Transient mesh, (i) Fine transient mesh, and (j) Very fine transient mesh [27].

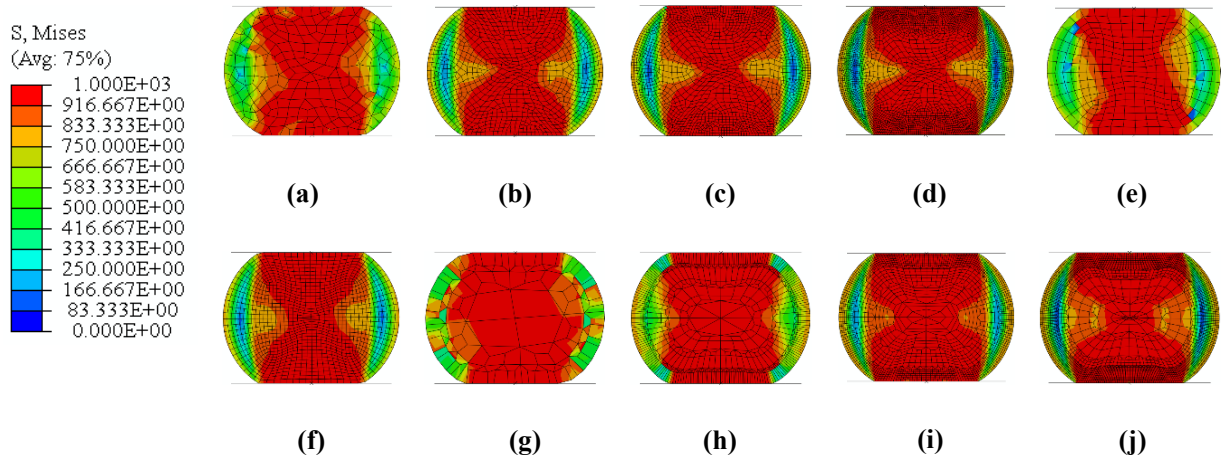

Fig. 3. Stress distribution during mesh sensitivity analysis: (a) Coarse free mesh, (b) Medium free mesh [12], (c) Fine free mesh, (d) Very fine free mesh, (e) Coarse structural mesh [13], (f) Fine structural mesh, (g) Coarse transient mesh [9], (h) Transient mesh, (i) Fine transient mesh, and (j) Very fine transient mesh [14].

for compaction. These numbers are enough to investigate inter-particle friction, die-wall friction, and the rearrangement of powders. The die walls and lower punch were rigid, and their displacement was restricted in all directions. A displacement boundary condition was imposed on the rigid upper punch. The displacement of the upper punch was used to calculate the instantaneous relative density. Experimental compression data measured the mechanical properties of Ti-6Al-4V, and the effect of superimposed ultrasonic vibration on this material was extracted from the authors' previous works [29,30]; and the material property of CP-Ti was extracted using the stress superposition theory from Ref. [31]. The inter-particle contacts and particle and die wall contacts were considered via a kinematic contact algorithm. The Coulomb friction theory was used as model. The inter-particle friction coefficient and the die wall friction coefficient with particles for both simulations of Ti-6Al-4V and CP-Ti powders were set at 0.28 and 0.4, respectively [32]. Regarding the large deformation of elements during compaction processes, the adaptive mesh technique was used with 60 frequencies. The effect of punch speed (simulation time) was investigated, and consequently, 0.05 s was selected for the simulation time.

To investigate the acoustic softening influence of ultrasonic vibrations in simulations, the Ti-6Al-4V alloy tensile test was performed under ultrasonic vibrations at two intensities of 100 and 340 W [17]. For CP titanium, the stress-strain curve under ultrasonic vibration was extracted from [18] for three vibrational amplitudes of 0, 5.6, and 6.4 μm. The relationship between the power (P) and amplitude of vibration (A) is as Eq. (1).

$$P = \frac{1}{2}A^2\omega^2\rho c \tag{1}$$

where ω is the angular frequency, ρ is the density, and c is the sound velocity in the material.

To apply the ultrasonic effect on the friction in simulations, the friction coefficient is assumed to be zero in the presence of ultrasonic vibrations.

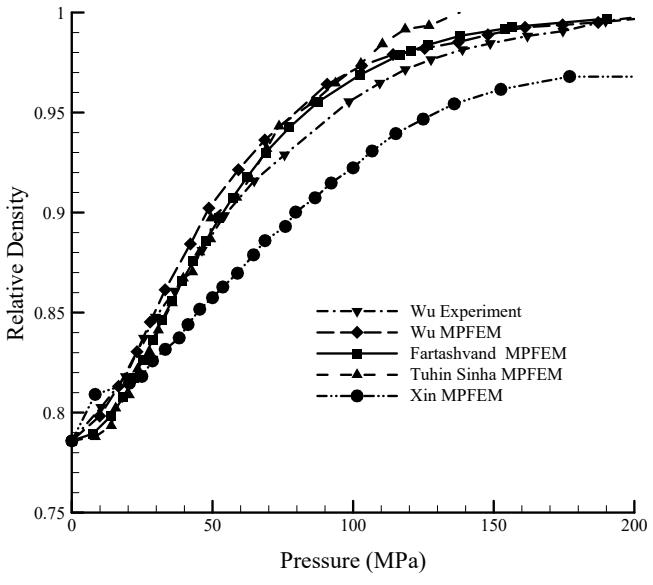

Fig. 4. Using relative density versus compression pressure to verify the simulation method.

3. Results and discussion

3.1. Comparison of ultrasonic effects on CP titanium and Ti-6Al-4V alloy

Compression pressure (P) plays a dominant role among many factors that can affect compaction. Here, P is referred to as the average pressure imparted to the upper punch. Fig. 5 shows the relationship between compaction pressure and upper punch displacement for three vibrational modes ((a)

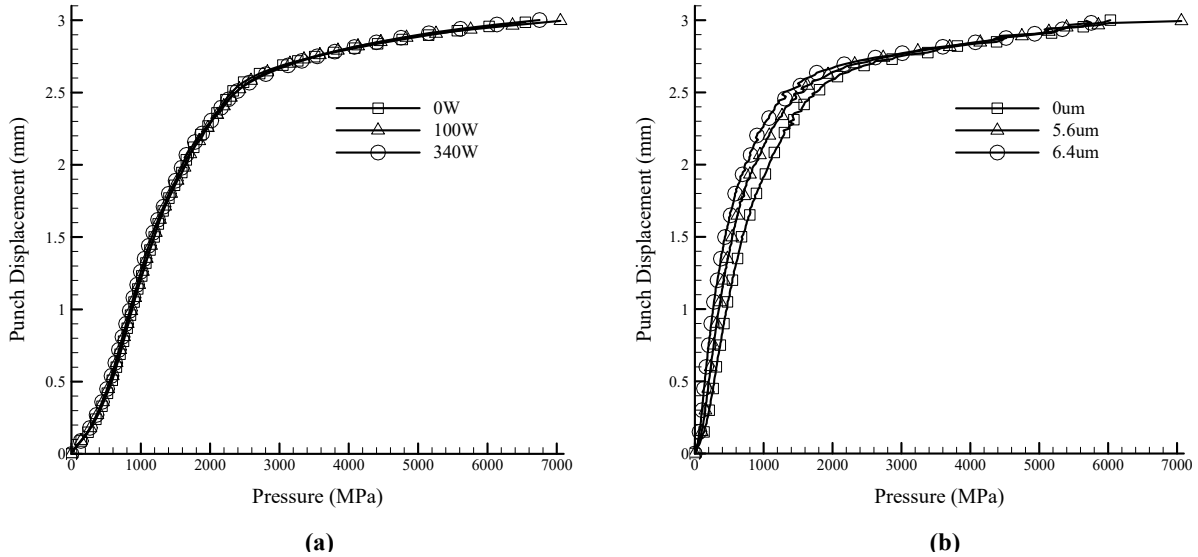

Fig. 5. Punch displacement versus compaction pressure for (a) Ti-6Al-4V alloy and (b) CP Titanium.

Ti-6Al-4V alloy and (b) CP titanium). As can be seen in both curves, moving the upper punch down first gradually increases the amount of pressure, but after about 2.5 mm displacement, the rate of increase in compaction force is increased. Also, the effect of ultrasonic vibrations on reducing the force required for powder compaction of CP titanium is greater than that of Ti-6Al-4V alloy.

Fig. 6 shows the relationship between pressure and relative density for Ti-6Al-4V and CP titanium. The relative density begins with the initial value of 0.78 and reaches full density under compaction pressure.

Investigation of the behavior of Ti-6Al-4V alloy in three ultrasonic intensities (Fig. 6(a)) showed that a relative density of 0.8 at ultrasonic powers of 0, 100, and 300 W is obtained at compaction pressures of 411, 401, and 388 MPa, respectively. Consequently, at a relative density of 0.8, the required pressure is reduced by about 10 MPa (2.4 %) and 13 MPa (5.5 %) by ultrasonic intensities of 100 and 300 W, respectively. In the case of CP titanium (Fig. 6(b)), the relative density of 0.8 at vibrational amplitudes of 0, 5.6, and 6.4 μm is obtained at compression pressures of 208, 153, and 105 MPa, respectively. Thus, at this relative density, the vibrational amplitudes of 5.6 and 6.4 μm reduced the required pressure to 55 MPa (26 %) and 103 MPa (49.5 %). Also, the ultrasonic effects on reducing required pressure in pure titanium are more significant than in titanium alloy. Therefore, the effect of acoustic softening led to reducing the required pressure, as the relative density of 0.92 for CP titanium was obtained at vibration amplitudes of 5.6 and 6.4 μm with lower pressures of 183 and 311 MPa, respectively, which indicates the effectiveness of ultrasonic vibrations in improving the densification behavior of the material.

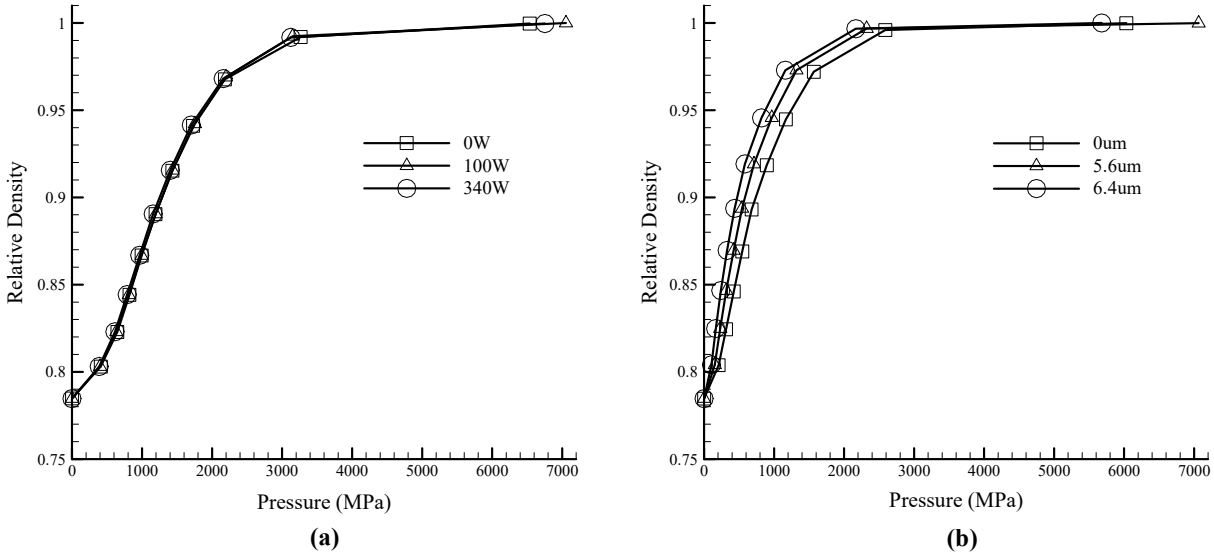

Fig. 6. Relative density versus compaction pressure for (a) Ti-6Al-4V alloy and (b) CP Titanium.

Compared to conventional compression (without ultrasonic), this pressure reduction is observed up to 99.7% relative density.

3.2. Macrostructure characterization during compaction

Figs. 7 and 8 indicate the evolution of morphology, local packing structure, and equivalent Von Mises stress for CP titanium and Ti-6Al-4V particles during compaction. The compression of Ti-6Al-4V needs more pressure than CP-Ti due to its higher strength. The pressure increases rapidly at the early stage of compaction. No apparent relative slip between particles for either case is observed due to the highly geometrical symmetry of the initial packing. It is also seen that at the early stages of compaction, the localized deformation of the particles leads to the formation of a stress chain; therefore, the particles are modeled as elastic-plastic.

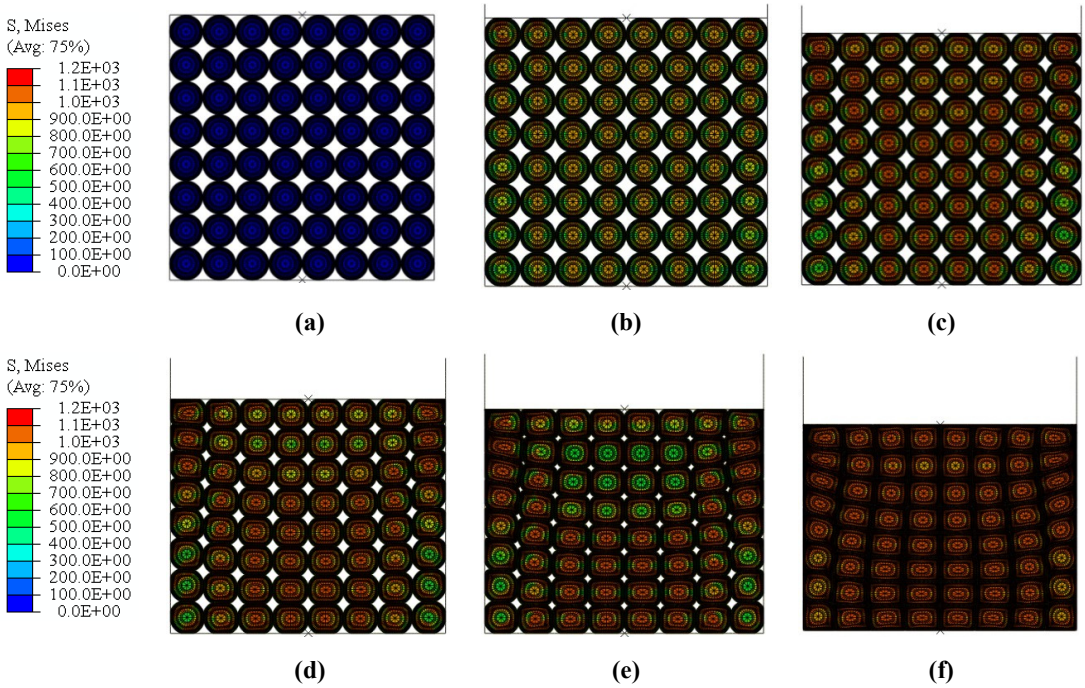

Fig. 7. Evolution of morphology, local packing structure, and equivalent Von Mises stress without ultrasonic vibration for Ti-6Al-4V during compaction in the punch displacement at (a) 0 mm, (b) 0.6 mm, (c) 1.2 mm, (d) 1.8 mm, (e) 2.4 mm, and (f) 3 mm.

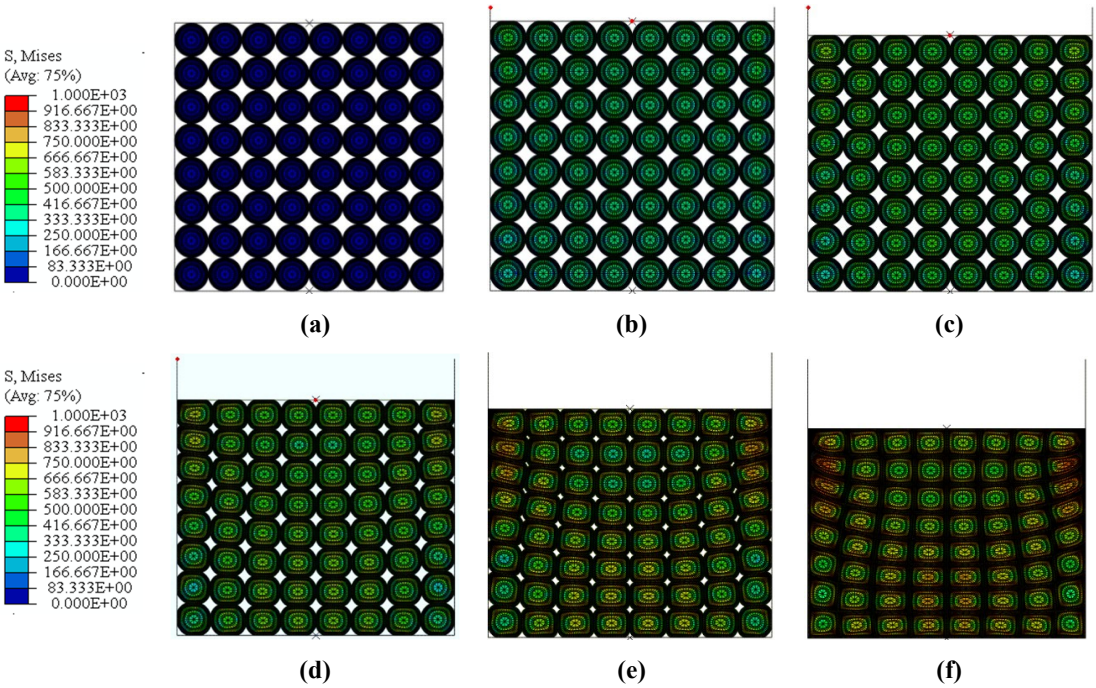

Fig. 8. Evolution of morphology, local packing structure, and equivalent Von Mises stress without ultrasonic vibration for CP titanium during compaction in the punch displacement at (a) 0 mm, (b) 0.6 mm, (c) 1.2 mm, (d) 1.8 mm, (e) 2.4 mm, and (f) 3 mm.

The plastic deformation begins when the Von Mises stress is equivalent to yield stress. Accordingly, it is observed that all the particles have plastic deformation, and they do not retain their original shape. So, with the further increase in the pressure, large plastic deformation of particles occurred, and in-plane forces between neighboring particles formed and increased. During this time, the contact between particles changes from point to arc. The significant plastic deformation results in the mass transfer of particles to fill adjacent low-pressure void area, causing densification.

The plastic deformation begins when the Von Mises stress is equivalent to yield stress. Accordingly, it is observed that all the particles have plastic deformation, and they do not retain their original shape. So, with the further increase in the pressure, large plastic deformation of particles occurred, and in-plane forces between neighboring particles formed and increased. During this time, the contact between particles changes from point to arc. The significant plastic deformation results in the mass transfer of particles to fill adjacent low-pressure void area, causing densification.

The compacted powders' relative density and uniform density distribution determine the green strength, sintering rate, final density, shrinkage, and distortion during sintering. The higher relative density of a powder compact results in higher green strength and higher relative density of its sintered part. Uniform density distribution causes lower shrinkage and distortion during sintering. So, reducing inter-particle voids causes good properties of the sintered parts. The particles in contact with the die walls deform non-uniformly due to the friction force, undergoing more deformation on one side and less stress on the other. After compaction, the shapes of particles in the compacts are nearly rectangular. From the comparison of Von Mises stress in morphological evolution on the compaction of pure titanium and Ti-6Al-4V alloy powders, it can be seen that ultrasonic vibrations lead to decreased stress. Also, increasing the amplitude and intensity of the ultrasonic reduces stress. These observations indicate the impact of ultrasonic acoustic softening.

The major benefit of the MPFEM model is its ability to obtain information regarding the local stress and strain state at the inter-particle contact area. To study the ultrasonic effect of friction reduction, friction was considered zero, and simulations were performed for both Ti-6Al-4V and CP titanium.

Figs. 9 and 10 show the distribution of equivalent Von Mises stress in the frictionless model for Ti-6Al-4V and CP -titanium, respectively. Removing the friction provides the possibility of the rotation and displacement of the particles and changes the position of the particles in the radial direction of the die. In contrast, there is no such rotation and displacement for compaction with the presence of friction. This phenomenon indicates how much friction affects the particle rearrangement stage. In other words, the rotating and rearrangement of the particles caused by removing friction led to increased compression capability. An investigation of the behavior of Ti-6Al-4V alloy showed that to achieve the relative density of 0.8, 0.89, and 0.99, the amount of pressure was reduced to 31, 525, and 814 MPa by removing friction. In the case of CP titanium, it was observed that the pressure was reduced to 25, 260, and 517 MPa by removing friction to achieve the relative density of 0.8, 0.89, and 0.99, respectively. Therefore, ultrasonic vibration can produce high-density green parts with a fairly uniform density distribution and a long tool lifetime. In Ti-6Al-4V, the effect of friction between particles and friction between particles and die walls was also investigated (each time, one was considered zero). The results indicate that removing friction between the particles is more effective than eliminating friction between particles and the die wall in reducing the required compaction pressure. So, ultrasonic vibrations have a beneficial influence in improving the densification behavior of the material.

4. Conclusion

The use of the multi-particle finite element model (MPFEM) offers an exciting insight into the compaction of particles. As a result, this model can address rearrangement, particle rotation, and large deformation to high relative densities.

In this research, a continuation of our previous published papers, the compression behavior of Ti-6Al-4V and CP titanium was investigated under a uniaxial longitudinal superimposed ultrasonic vibration condition. Ultrasonic vibration was modeled as acoustic softening in material properties and friction reduction. The following conclusions can be drawn from our results:

(a) It is observed that ultrasonic vibration decreases the required pressure for compaction. This enhancement in CP titanium was greater than in Ti-6Al-4V alloy.

(b) A higher ultrasonic intensity and amplitude will increase its effectiveness in reducing compaction pressure.

(c) The rotating and rearrangement of the particles caused by the reduction of friction leads to increased compression capability.

(d) The results indicate that removing friction between the particles is more effective than eliminating friction between particles and the die wall in reducing the required compaction pressure.

Acknowledgement

The authors express their sincere appreciation to Dr. Yunes

Alizadeh and Dr. Nader Parvin for their help and support. Thanks should also be given to the Farasou Tajhiz Iranian Co. No for funding.

Disclosure statement

No potential conflict of interest was reported by the authors.

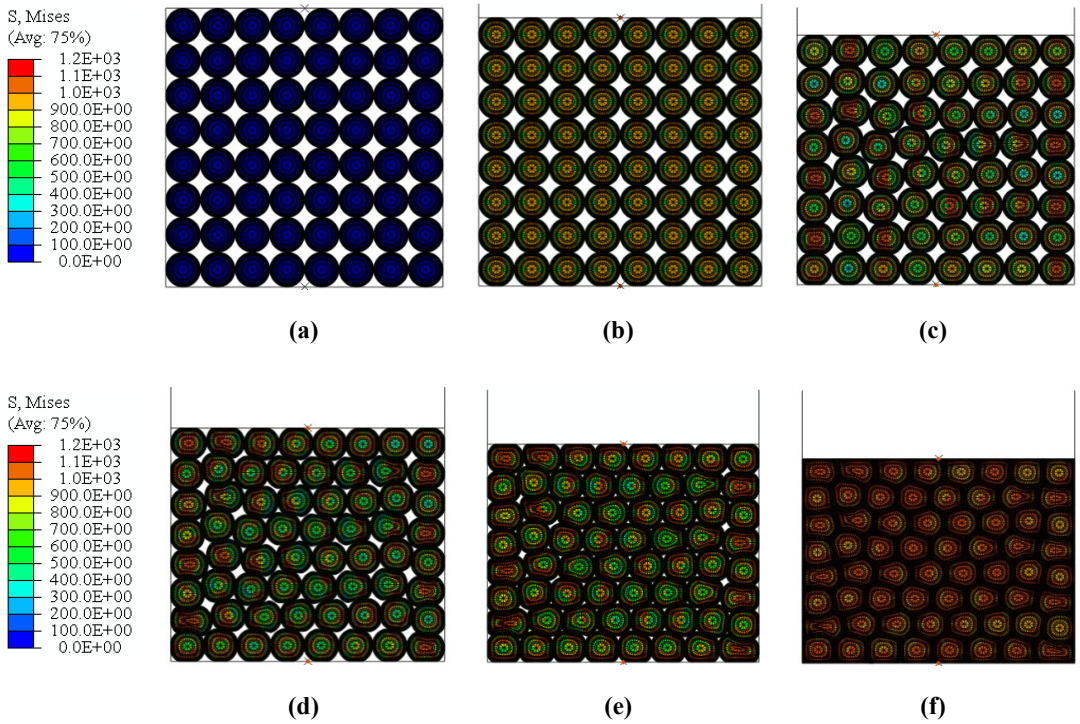

Fig. 9. Evolution of morphology, local packing structure, and equivalent Von Mises stress for Ti-6Al-4V alloy during frictionless compaction in the punch displacement at (a) 0 mm, (b) 0.6 mm, (c) 1.2 mm, (d) 1.8 mm, (e) 2.4 mm, and (f) 3 mm.

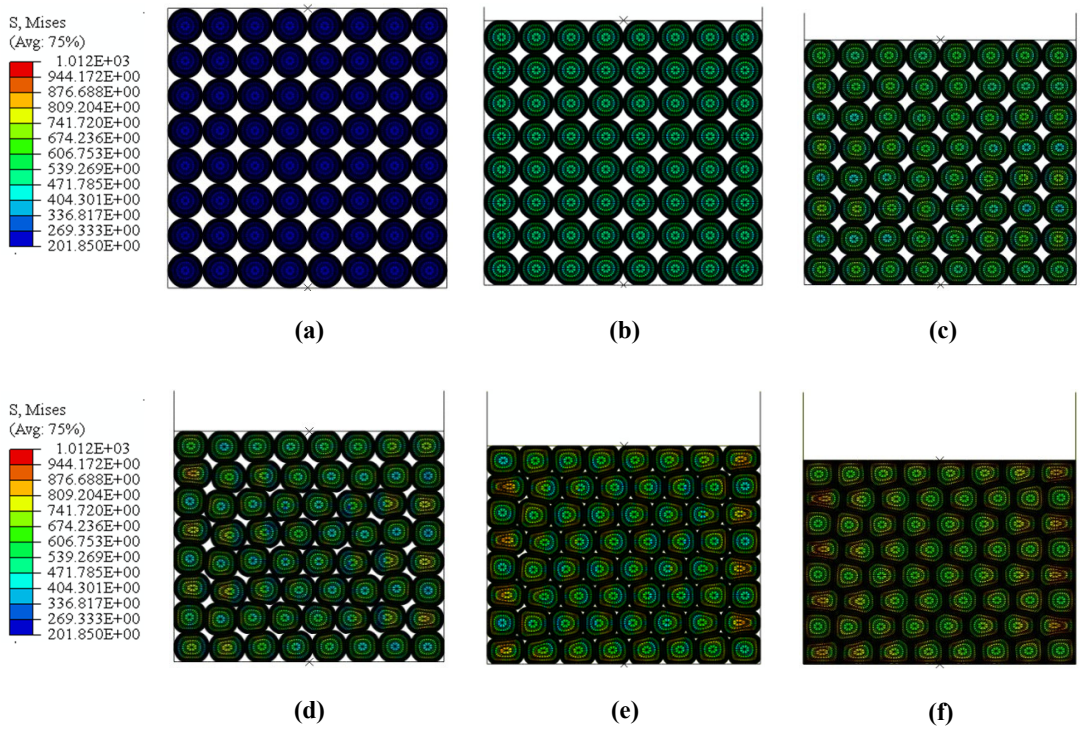

Fig. 10. Evolution of morphology, local packing structure, and equivalent Von Mises stress for CP titanium during frictionless compaction in the punch displacement at (a) 0 mm, (b) 0.6 mm, (c) 1.2 mm, (d) 1.8 mm, (e) 2.4 mm, and (f) 3 mm.

References

[1] Donachie, M. J. (2000). *Titanium: A Technical Guide* (2nd ed.). ASM International. https://doi.org/10.31399/asm.tb.ttg2.9781627082693

[2] Amini, S. Farzin, M., & Mohammadi, A. (2023). An Experimental Study on Ultrasonic-assisted Hot Incremental Sheet Metal Forming of Ti–6Al–4V. *Iranian Journal of Science and Technology, Transactions of Mechanical Engineering, 47*, 1923-1935. https://doi.org/10.1007/s40997-023-00602-8

[3] Esteban, P. G., Thomas, Y., Baril, E., Ruiz-Navas, E. M., & Gordo, E. (2011). Study of Compaction and Ejection of Hydrided-Dehydrided Titanium Powder. *Metals and Materials International, 17*, 45-55. https://doi.org/10.1007/s12540-011-0207-z

[4] Liu, Y., Chen, L. F., Tang, H. P., Liu, C. T., Liu, B., & Huang, B. Y. (2006). Design of Powder Metallurgy Titanium Alloys and Composites, *Materials Science and Engineering: A, 418*(1-2), 25-35. https://doi.org/10.1016/j.msea.2005.10.057

[5] Qian, M., Froes, F. H. (2015). *Titanium Powder Metallurgy Science, Technology and Applications* (1st ed.). Elsevier. https://doi.org/10.1016/C2013-0-13619-7

[6] Fartashvand, V., Abdullah, A., & Sadough Vanini, S. A. (2017). Effects of High Power Ultrasonic Vibration on the Cold Compaction of Titanium. *Ultrasonics Sonochemistry, 36*, 155-161. https://doi.org/10.1016/j.ultsonch.2016.11.017

[7] Fartashvand, V., Abedini, R., & Abdullah, A. (2022). Influence of Ultrasonic Vibrations on the Properties of Press-and-Sintered Titanium. *Proceedings of the Institution of Mechanical Engineers, Part B: Journal of Engineering Manufacture, 236*(11), 1518-1525. https://doi.org/10.1177/09544054221078386

[8] Abedini, R., Fartashvand, V., Abdullah, A., & Alizadeh, Y. (2022). Evaluation of Process Parameters and Ultrasonic Vibration in Hot Pressing of Metal Powders. *Materials Science and Engineering: B, 281*, 115731. https://doi.org/10.1016/j.mseb.2022.115731

[9] Dong, S. & Dapino, M. J. (2014). Elastic–Plastic Cube Model for Ultrasonic Friction Reduction via Poisson's Effect. *Ultrasonics, 54*(1), 343-350. https://doi.org/10.1016/j.ultras.2013.05.011

[10] Meng, B., Cao, B. N., Wan, M., Wang, C. J., & Shan, D. B. (2019). Constitutive Behavior and Microstructural Evolution in Ultrasonic Vibration Assisted Deformation of Ultrathin Superalloy Sheet. *International Journal of Mechanical Sciences, 157-158*, 609-618. https://doi.org/10.1016/j.ijmecsci.2019.05.009

[11] Sancin, P., Caputo, O., Cavallari, C., Passerini, N., Rodriguez, L., Cini, M., & Fini, A. (1999). Effects of Ultrasound-Assisted Compaction on Ketoprofen/ Eudragit S100 Mixtures. *European Journal of Pharmaceutical Sciences, 7*(3), 207-213. https://doi.org/10.1016/S0928-0987(98)00022-0

[12] Abedini, R., Abdullah, A., Alizadeh, Y., & Fartashvand V. (2017). A Roadmap for Application of High Power Ultrasonic Vibrations in Metal Forming. *Modares Mechanical Engineering, 16*(10), 323-334.

[13] Abedini, R., Fartashvand, V., Abdullah, A., & Alizadeh, Y. (2024). Finite Element Modelling of Ultrasonic Assisted Hot Pressing of Metal Powder. *Mechanics of Time-Dependent Materials, 28*, 3263-3278. https://doi.org/10.1007/s11043-024-09735-y

[14] Kumar, N., Bharti, A., & Saxena, K. K. (2021). A Re-Investigation: Effect of Powder Metallurgy Parameters on the Physical and Mechanical Properties of Aluminium Matrix Composites. *Materials Today: Proceedings, 44*(Part 1), 2188-2193. https://doi.org/10.1016/j.matpr.2020.12.351

[15] Kaseb, I., Moazami-Goudarzi, M., & Abbasi, A. R. (2019). Effect of Particle Size on the Compressibility and Sintering of Titanium Powders. *Iranian Journal of Materials Forming, 6*(2), 42-51. https://doi.org/10.22099/ijmf.2019.34264.1134

[16] Zahraee, S. M. (2016). Experimental Investigation of Metal Powder Compaction without Using Lubricant. *Journal of Particle Science and Technology, 2*(3), 141-149. https://doi.org/10.22104/jpst.2016.445

[17] Procopio, A. T., & Zavaliangos, A. (2005). Simulation of Multi-Axial Compaction of Granular Media from Loose to High Relative Densities. *Journal of the Mechanics and Physics of Solids, 53*(7), 1523-1551. https://doi.org/10.1016/j.jmps.2005.02.007

[18] Huang, F., An, X., Zhang, Y., & Yu, A. B. (2017). Multi-Particle FEM Simulation of 2D Compaction on Binary Al/SiC Composite Powders. *Powder Technology, 314*, 39-48. https://doi.org/10.1016/j.powtec.2017.03.017

[19] Korim, N. S., & Hu, L. (2020). Study the Densification Behavior and Cold Compaction Mechanisms of Solid Particles-Based Powder and Spongy Particles-Based Powder Using a Multi-Particle Finite Element Method. *Materials Research Express, 7*(5), 056509. https://doi.org/10.1088/2053-1591/ab8cf6

[20] Lee, K. H., Lee, J. M., & Kim, B. M. (2009). Densification Simulation of Compacted Al Powders Using Multi-Particle Finite Element Method. *Transactions of Nonferrous Metals Society of China, 19*(Suppl. 1), s68-s75. https://doi.org/10.1016/S1003-6326(10)60247-6

[21] Feng, Y., Mei, D., & Wang, Y. (2019). Cohesive Zone Method Based Multi-Particle Finite Element Simulation of

Compaction Densification Process of Al and NaCl Laminar Composite Powders. J*ournal of Physics and Chemistry of Solids, 134*, 35-42. https://doi.org/10.1016/j.jpcs.2019.05.020

[22] Han, P., An, X., Wang, D., Fu, H., Yang, X., Zhang, H. & Zou, Z. (2020). MPFEM Simulation of Compaction Densification Behavior of Fe-Al Composite Powders with Different Size Ratios. *Journal of Alloys and Compounds, 741*, 473-481. https://doi.org/10.1016/j.jallcom.2018.01.198

[23] Zhou, J., Zhu, C., Zhang, W., Ai, W., Zhang, X., & Liu, X. (2020). Experimental and 3D MPFEM Simulation Study on the Green Density of Ti–6Al–4V Powder Compact During Uniaxial High Velocity Compaction. *Journal of Alloys and Compounds,* 817, 153226. https://doi.org/10.1016/j.jallcom.2019.153226

[24] Xu, L., Wang, Y., Li, C., Ji, G., & Mi, G.(2021). MPFEM Simulation on Hot-Pressing Densification Process of SiC Particle/6061Al Composite Powders. *Journal of Physics and Chemistry of Solids, 159*, 110259. https://doi.org/10.1016/j.jpcs.2021.110259

[25] Gustafsson, G., Häggblad, H. A., & Jonsén, P. (2013). Multi-Particle Finite Element Modelling of the Compression of Iron Ore Pellets with Statistically Distributed Geometric and Material Data. *Powder Technology, 239*, 231-238. https://doi.org/10.1016/j.powtec.2013.02.005

[26] Zhang, Y. X., An, X. Z., & Zhang, Y. L. (2015). Multi-Particle FEM Modeling on Microscopic Behavior of 2D Particle Compaction. *Applied Physics A, 118*, 1015-1021. https://doi.org/10.1007/s00339-014-8861-x

[27] Wu, W., Jiang, G., Wagoner, R. H., & Daehn, G. S. (2000). Experimental and Numerical Investigation of Idealized Consolidation. Part 1: Static Compaction. *Acta Materialia, 48*(17), 4323-4330. https://doi.org/10.1016/S1359-6454(00)00206-8

[28] Xin, X. J., Jayaraman, P., Daehn, G. S., & Wagoner, R. H. (2003). Investigation of Yield Surface of Monolithic and Composite Powders by Explicit Finite Element Simulation. *International Journal of Mechanical Sciences, 45*(4), 707-723. https://doi.org/10.1016/S0020-7403(03)00107-3

[29] Fartashvand, V., Abdullah, A., & Sadough Vanini, S. A. (2017). Investigation of Ti-6Al-4V Alloy Acoustic Softening. *Ultrasonics Sonochemistry, 38*, 744-749. https://doi.org/10.1016/j.ultsonch.2016.07.007

[30] Sadeghi, M., Fartashvand, V., Abdullah, A., Fallahi Arezoodar, A. R., & Abedini, R. (2022). Experimental Investigation of Vibrational Mode Shape Influence on Compression Behaviour of Ti-6Al-4V Alloy Under Superimposed Ultrasonic Vibration. *Journal of Solid and Fluid Mechanics, 12*(4), 55-68. https://doi.org/10.22044/jsfm.2022.11100.3452

[31] Zhou, H., Cui, H., Qin, Q. H., Wang, H., & Shen, Y.(2017). A Comparative Study of Mechanical and Microstructural Characteristics of Aluminium and Titanium Undergoing Ultrasonic Assisted Compression Testing. *Materials Science and Engineering: A, 682*, 376-388. https://doi.org/10.1016/j.msea.2016.11.021

[32] Boyer, R., Welsch, G., & Collings, E. W. (1994). *Material Properties Handbook: Titanium Alloys*. ASM International.

Additional information

Correspondence and requests for materials should be addressed to V. Fartashvand.

HOW TO CITE THIS ARTICLE

Fartashvand, V.; Abedini, R.; Khanmohammadi, R.; Abdullah, A.; Parvin, N.; Ultrasonic assisted cold compaction of CP titanium and Ti-6Al-4V alloy*, J. Part. Sci. Technol. 10(2024) 87-96.*

DOI: 10.22104/jpst.2024.7089.1262
URL: https://jpst.irost.ir/article_1472.html